Hydrogenation of Levoglucosenone to Renewable Chemicals*

Siddarth H. Krishna, Daniel J. McClelland, Quinn A. Rashke, James A. Dumesic, George W. Huber†

Abstract

We have studied the hydrogenation of levoglucosenone (LGO) to dihydrolevoglucosenone (Cyrene), levoglucosanol (Lgol), and tetrahydrofurandimethanol (THFDM) and elucidated the reaction network over supported palladium catalysts. At low temperature (40°C) over a Pd/Al_2O_3 catalyst, LGO can be selectively hydrogenated to Cyrene. At intermediate temperatures (100°C) over a Pd/Al_2O_3 catalyst, Cyrene can be selectively hydrogenated to Lgol, with an excess of the exo-Lgol isomer produced over the endo-Lgol isomer. At higher temperatures (150°C) over a bifunctional Pd/SiO_2-Al_2O_3 catalyst, Lgol is converted to THFDM in 58% selectivity, with 78% overall selectivity to 1,6-hexanediol precursors. The ratio of cis-THFDM relative to trans-THFDM is approximately 2.5, and this ratio is independent of the Lgol feed stereoisomer ratio. Tetrahydropyran-2-methanol-5-ketone (THP2M5one) and tetrahydropyran-2-methanol-5-hydroxyl (THP2M5H) are side-products of Lgol hydrogenolysis, but neither of these species are precursors to THFDM.

1. Introduction

In recent years, lignocellulosic biomass has gained interest as a renewable feedstock for the production of high-value oxygenated chemicals.[1,2] We have recently shown that levoglucosenone (LGO) can be produced from cellulose in 50% yield using a polar aprotic solvent and sulfuric acid catalyst.[3] This strategy uses relatively mild conditions (210°C, 20 mM H_2SO_4) and avoids complex separation processes such as the vacuum pyrolysis approach used by Kawamoto et al.[4] Due to these improvements over the conventional pyrolysis approach,[4, 5] LGO has the potential to become a biomass-derived platform molecule, thereby broadening the opportunities for conversion of cellulose to fuels and chemicals.

As shown in Scheme 1, LGO can be hydrogenated into a wide variety of chemicals. At low temperatures (25-60°C) over a Pd/C catalyst, LGO is hydrogenated into Cyrene (dihydrolevoglucosenone), a non-toxic solvent with similar properties to environmentally harmful solvents such as N-methylpyrrolidone.[6-8] DuPont has reported that LGO can be hydrogenated to levoglucosanol (Lgol) followed by hydrogenolysis to tetrahydrofurandimethanol (THFDM) in 84% yield over a Pt/C catalyst.[9] THFDM can be further upgraded to 1,6-hexanediol in >80% yield using a bifunctional catalyst that contains metal and acid sites.[10-13] Lgol contains three chiral centers and is a potential platform molecule for chiral products relevant to the fine chemicals and pharmaceuticals industry.[14] THFDM is an α,ω-diol with the potential to be a polymer precursor similar to existing α,ω-diols in the market.[2,15] 1,6-hexanediol is a commodity chemical used in polyurethanes, coatings, and adhesives.[12,16-18] While the biomass-derived intermediate 5-

* Electronic supplementary information (ESI) available: Gaussian DFT calculations; ^{13}C NMR of reaction products; CO chemisorption data; synthesis of reaction intermediates; product deconvolution methods; solvent degradation data; and catalyst recycling data.

† Department of Chemical and Biological Engineering, University of Wisconsin-Madison, Madison, WI 53706, USA. Email: gwhuber@wisc.edu.

hydroxymethylfurfural (HMF) can also be hydrogenated into THFDM and 1,6-hexanediol,[12,19-21] LGO upgrading could provide a new route to these chemicals as well as Cyrene and Lgol. Furthermore, the fundamental chemistry of LGO hydrogenation and hydrogenolysis has not been explored in detail in the literature.

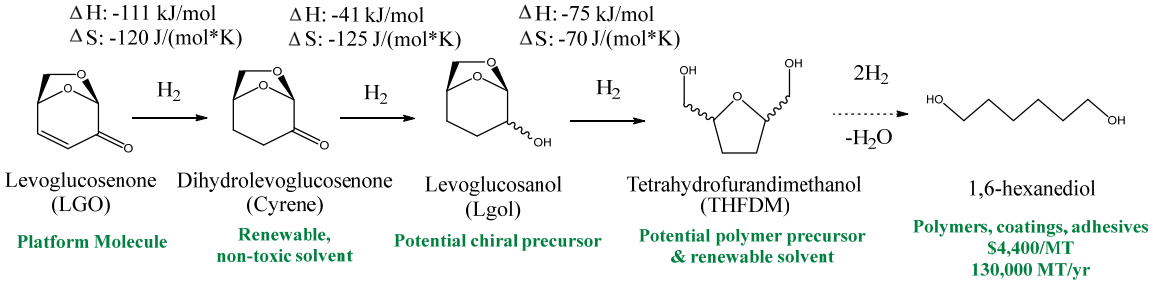

Scheme 1: Levoglucosenone hydrogenation. Enthalpies and entropies of reaction were estimated using Gaussian DFT calculations (see Supplemental Information).

Herein, we study the hydrogenation of LGO over supported palladium catalysts. We elucidate the reaction network and demonstrate catalysts and conditions suitable to produce Cyrene, Lgol, or THFDM depending on which products are desired. We also gain mechanistic insights from investigations of the effect of metal acid sites and selectivity as a function of conversion. Our results reveal the chemistry underlying the hydrogenation of LGO, and provide directions for designing catalytic systems to optimize the production of several renewable chemicals, including green solvents and polymer precursors, from lignocellulosic biomass.

2. Experimental

LGO (98%, Apollo Scientific), Cyrene (99%, Apollo Scientific), THFDM (98%, Alfa Chemicals), tetrahydrofuran (THF) stabilized with butylated hydroxytoluene (BHT) (99.9%, Acros Organics), and $Pd(NO_3)$ solution (10% in 10% HNO_3, Sigma Aldrich), were used as received. 5% Pd/C and low-soda γ-Al_2O_3 were purchased from Strem Chemicals. 1% Pd/C, Davisil SiO_2, and Grade 135 amorphous SiO_2-Al_2O_3 (Si-Al) were purchased from Sigma Aldrich.

2.1. Catalyst synthesis methods

Palladium catalysts supported on Al_2O_3 and Si-Al were synthesized by incipient wetness impregnation (IWI) of a 10% $Pd(NO)_3$ precursor onto the appropriate support. After impregnation, catalysts were dried overnight in an oven at 110°C. The catalysts were then calcined in flowing air at 400°C followed by reduction in flowing H_2 at 260°C and passivation in 1% O_2/He at room temperature.

2.2. Catalyst characterization methods

Carbon monoxide (CO) chemisorption was carried out in a Micromeritics ASAP2020C instrument. 100 mg of the catalyst was loaded into a glass reactor. Catalysts were degassed followed by *in situ* reduction in flowing H_2 at 400°C and sample evacuation. The CO chemisorption measurement was conducted at 35°C, and repeated after subsequent evacuation to acquire the reversible CO uptake. The irreversible CO uptake was calculated by subtracting the total uptake in the first measurement from the reversible uptake in the second measurement.

2.3 Reaction Studies

Reactions were carried out in 45 or 75 mL Parr Hastelloy high-pressure batch reactors. A magnetic stir bar and appropriate amount of catalyst and feedstock were added to the reactor. The reactor was purged four times with 500 psi H_2, followed by pressurizing to 500 psi H_2. The heat-up time was 10-15 minutes. The reaction mixture was stirred at 750 rpm. After the appropriate time, the reactor was quenched in ice water, depressurized, and opened. The reaction products were filtered using a 0.2 μm PTFE (polytetrafluoroethylene) syringe filter prior to analysis.

For LGO hydrogenation at low temperature (40°C), catalysts were pre-reduced at 100°C in flowing H_2 and loaded into Parr reactors in a glovebox to avoid exposure to air. For reactions at higher temperature (>40°C), passivated catalysts were loaded directly into the reactor without pre-reduction.

Dip-tube experiments were carried out with 60 mL reaction mixture in a 75 mL Parr batch reactor equipped with a 1/8-inch dip-tube. During sampling, 0.6 mL was purged followed by 0.6 mL collected for analysis. Purging was done to remove dip-tube liquid collected at earlier reaction times. A stainless steel filter (500-mesh) was used to prevent solids from entering the dip-tube. After each sample, the reactor was re-pressurized with H_2.

2.4 Product analysis methods

2.4.1 GC

Products were quantified using a Shimadzu Gas Chromatograph equipped with a Flame Ionization Detector (FID) with liquid injection. A Restek RTX-VMS capillary column (Length: 30 m, ID: 0.25 mm, film thickness: 1.4 μm) was used. The injection port and FID were maintained at 240°C. The injection volume was 1 μL and a split ratio of 50 was used. The column temperature ramp was as follows: hold 1 min at 40°C, ramp 10°C/min to 180°C, ramp 3°C/min to 240°C, hold 5 min at 240°C.

Because Lgol, THP2M5one (tetrahydropyran-2-methanol-5-ketone), and THP2M5H (tetrahydropyran-2-methanol-5-hydroxyl) are not commercially available, these compounds were synthesized and their identities were confirmed by ^{13}C NMR. Lgol and THP2M5one were assumed to have GC sensitivities equal to the average sensitivity of LGO and Cyrene. THP2M5H and 2MTHFA (2-methyl-tetrahydrofurfuryl alcohol) were assumed to have GC sensitivities equal to that of THFDM. 2MTHFA was identified using a Shimadzu Gas Chromatograph equipped with a Quadrupole Mass Spectrometer with liquid injection (GCMS-QP2010S). The ion source and interface temperatures were set to 200°C, and a solvent cut was used to avoid introducing the solvent into the MS.

It was observed that cis-THFDM was overlapped by THP2M5one in the GC. THP2M5one was quantified independently using HPLC, and the concentration of cis-THFDM was calculated by subtracting the known concentration of THP2M5one from the total concentration of these two species in the GC. It was also observed that trans-THFDM was overlapped by one of the stereoisomers of THP2M5H in the GC. The relative concentrations of cis-THFDM, trans-THFDM, and the two stereoisomers of THP2M5H were acquired by quantitative ^{13}C NMR. For experiments with sampling over time, the concentration of trans-THFDM at earlier reaction times was calculated from the cis-THFDM concentration, assuming that the cis/trans ratio is not a function of conversion. This assumption was validated by running the Lgol hydrogenolysis reaction to high

conversion as well as intermediate conversion and confirming that the THFDM cis/trans ratio was similar in both cases. Then, the concentration of the overlapped isomer of THP2M5H at earlier time points was calculated by subtracting the known concentration of trans-THFDM from the total concentration of these two species in the GC. Product deconvolution using a combination of GC, NMR, and HPLC is discussed in detail in the Supplemental Information.

2.4.2. HPLC

THP2M5one was quantified using a Shimadzu high performance liquid chromatograph (HPLC) with a BioRad Aminex 87H column and 5 mM H_2SO_4 mobile phase. The column was operated at a flow rate of 0.6 mL/min and a temperature of 30ºC. A photodiode array (UV) detector was used at a UV wavelength of 206 nm.

2.4.3 NMR

Quantitative ^{13}C NMR spectra were collected on a Bruker Avance 500 MHz spectrometer at room temperature, using an inverse-gated decoupling pulse sequence with a 30º pulse. The ^{13}C NMR spectra were absolute-referenced to the associated ^{1}H NMR spectra. Unless otherwise indicated, 256 scans were used, with an acquisition time of 1 sec and a relaxation delay of 15 sec. Reaction products exo-Lgol, endo-Lgol, cis-THFDM, trans-THFDM, THP2M5one, and the two stereoisomers of THP2M5H were identified using ^{13}C NMR. Samples were prepared for analysis by evaporating the THF solvent from 5-10 mL of sample, then adding 1-3 mL of d_6-DMSO. ^{13}C NMR spectra for these compounds are provided in the Supplemental Information.

3. Results and Discussion

3.1. Hydrogenation of LGO to Cyrene

LGO hydrogenation to Cyrene was carried out over a 0.4 wt% Pd/Al_2O_3 catalyst. THF was selected as the reaction solvent because this solvent was effective in our previous work for cellulose dehydration to LGO.[3] As shown in Figure 1, at low temperature (40 °C), LGO was hydrogenated to Cyrene in 100% selectivity. These results agree with the findings of Clark et al., who observed quantitative conversion of LGO to Cyrene over a Pd/C catalyst at room temperature.[6] Levoglucosenol, the unsaturated alcohol resulting from selective hydrogenation of the C=O bond of LGO, was not observed at any time. Similarly, Ronzon et al. found that complete C=C bond hydrogenation occurred prior to C=O hydrogenation in the hydrogenation of 2-cyclohexenone (a molecule with the same 2-enone functionality as is present in LGO) over Rh/SiO_2 catalysts.[22] In general, hydrogenation of C=C bonds is thermodynamically favored compared to hydrogenation of C=O bonds.[23] Based on the data in Figure 1, the initial turnover frequency (TOF) for LGO hydrogenation at these conditions was 345 mol Cyrene per mol surface Pd per min. Catalyst recycling data suggest that this catalyst undergoes deactivation under these conditions (Supplemental Information, Figure S6).

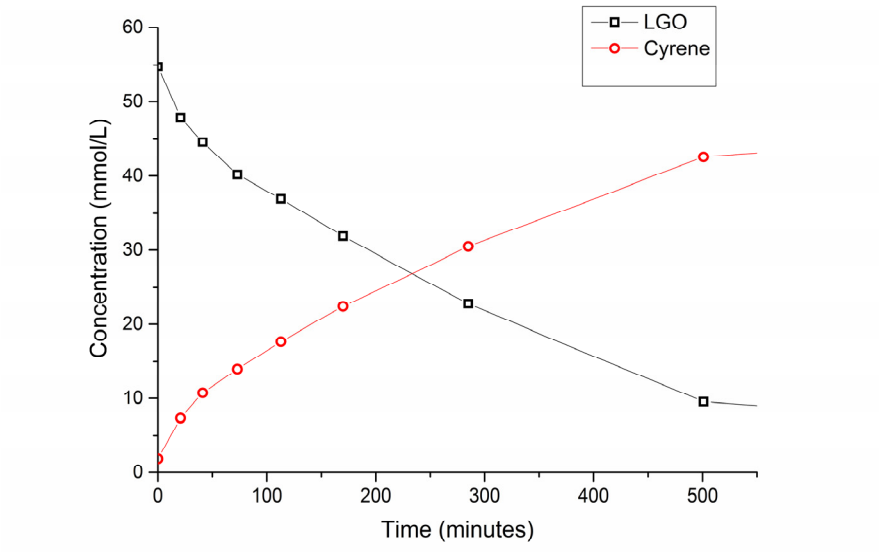

Figure 1. Hydrogenation of LGO over 1.75 mg 0.4 wt% Pd/Al_2O_3 (17.5 mg diluted 10x in SiO_2) in a batch reactor with dip-tube sampling. Conditions: 40°C, 500 psi H_2, 60 mL 55 mM LGO feed in THF. Solid lines between points are visual aids.

3.2. Hydrogenation of Cyrene to Lgol

Cyrene hydrogenation to Lgol was investigated at higher temperature (100°C) and at higher catalyst amounts compared to LGO hydrogenation. As shown in Figure 2, under these conditions Cyrene was hydrogenated to Lgol in 100% selectivity. Based on the data in Figure 2, the initial turnover frequency (TOF) for Cyrene hydrogenation at these conditions was 8.5 mol Lgol per mol surface Pd per min. Catalyst recycling data suggest that this catalyst undergoes more significant deactivation under these conditions compared to the case of LGO hydrogenation (Supplemental Information, Figure S7). An excess of the exo-Lgol isomer was produced over the endo-Lgol isomer (exo/endo = 4.6), and the stereoisomer ratio was not a function of conversion. Augustine argued that in the stereoselective hydrogenation of prochiral ketones (i.e., ketones which already contain stereocenters), hydrogen atom addition from the less hindered direction should be kinetically favored.[24] We hypothesize that the observed excess of exo-Lgol results from preferential hydrogen atom addition to the ketone group of Cyrene from the opposite side as the anhydro-bridge.[5] Similarly, Zanardi et al. found that the C=O bond of LGO was selectively reduced to the exo-alcohol when sodium borohydride was used as the reductant.[14] Based on our results, we have proposed the reaction network for LGO hydrogenation to Lgol shown in Scheme 2.

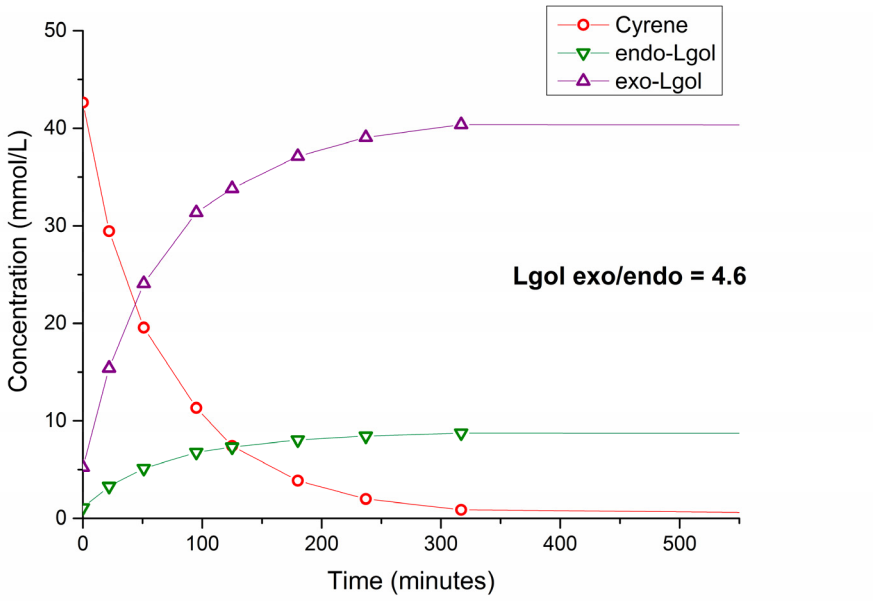

Figure 2. Hydrogenation of Cyrene over 150 mg 0.4 wt% Pd/Al_2O_3 in a batch reactor with dip-tube sampling. Conditions: 100°C, 500 psi H_2, 60 mL 55 mM Cyrene in THF feed. Solid lines between points are visual aids.

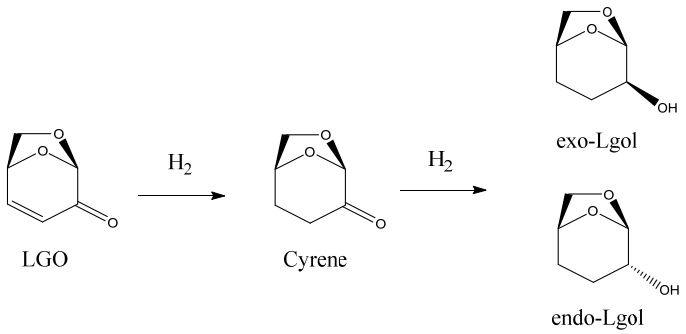

Scheme 2: Proposed reaction network for LGO hydrogenation.

The ratio of exo-Lgol to endo-Lgol in Cyrene hydrogenation for different supported palladium catalysts is shown in Table 1. While the conversion values were different for the different experiments in Table 1, Figure 2 indicates that the stereoselectivity does not depend on conversion. Cyrene hydrogenation over a 1 wt% Pd/C catalyst resulted in exo/endo = 2.3, while hydrogenation over a 0.4 wt% Pd/Al_2O_3 catalyst resulted in exo/endo = 4.6. Since the stereoisomer ratio varies with the catalyst used, it is governed by kinetics rather than thermodynamics. The stereoisomer ratio is a function of the catalyst support, as indicated by the stereoisomer ratio over 1% and 5% Pd/C catalysts (1.7-2.3) versus 0.4% and 5% Pd/Al_2O_3 catalysts (4.6-4.7) and the 1% Pd/Si-Al catalyst (3.5). Comparing 0.4 wt% Pd/Al_2O_3 (~2 nm particles, as shown in Table S1) with 5 wt% Pd/Al_2O_3 (~10 nm particles), the stereoisomer ratios were similar, suggesting that the stereoisomer ratio is not affected by changes in the particle size. Additionally, as shown in Table 1, the

stereoisomer ratios over the 0.4 wt% Pd/Al_2O_3 were comparable at temperatures of 100°C and 150°C. This result suggests that the apparent activation energies for exo-Lgol and endo-Lgol formation are similar. While the stereoisomer ratio was observed to change with the choice of support, the underlying reason for this dependence is not known at present.

Table 1. Cyrene Hydrogenation –Stereoisomer Ratio

Catalyst	Temperature [°C]	Conversion [%]	Lgol Isomer Ratio (exo/endo)
1% Pd/C	100	71	2.3
5% Pd/C	100	100	1.7
0.4% Pd/Al_2O_3	100	0-100*	4.6
0.4% Pd/Al_2O_3	150	100	4.4
5% Pd/Al_2O_3	100	100	4.7
1% Pd/Si-Al	100	95	3.5

Conditions: 500 psi H_2, 10 mL 55 mM Cyrene in THF feed, 50 mg cat, 3h reaction time.
**Taken from Figure 2.*

3.3. Hydrogenolysis of Lgol to THFDM

The hydrogenolysis of Lgol to THFDM involves a ring-rearrangement to form the 5-membered ring of THFDM. Using a Pd/Si-Al catalyst at 150°C, 58% selectivity towards THFDM was achieved at 90% Lgol conversion, as shown in Table 2. A ~2.8:1 excess of cis-THFDM was produced over trans-THFDM. In contrast, when THFDM is produced from HMF hydrogenation, the product mixture has been reported to comprise predominantly (>95%) the cis-THFDM isomer, most likely because the C=C bonds in the furan ring of HMF would be hydrogenated from the same direction.[12,25] THFDM can be converted into 1,2,6-hexanetriol followed by further upgrading to 1,6-hexanediol.[10-13] We expect that both cis-THFDM and trans-THFDM can be upgraded to 1,6-hexanediol.

The major side-products of Lgol hydrogenolysis were THP2M5H and 2MTHFA, as shown in Scheme 3. Both of these species contain two stereoisomers, but the stereochemistry could not be assigned due to the low yields of these products. DuPont also reported THP2M5H as a minor product of Lgol hydrogenolysis.[9] Although we do not know of any literature studies of THP2M5H hydrogenolysis, we expect that THP2M5H, like THFDM, can be upgraded to 1,2,6-hexanetriol through ring-opening at the C-O bond adjacent to the hydroxymethyl group. Therefore, the overall selectivity to 1,6-hexanediol precursors THFDM and THP2M5H is 78%. We note that degradation of the THF solvent in the presence of Lgol is negligible under these reaction conditions, as presented in the Supplemental Information.

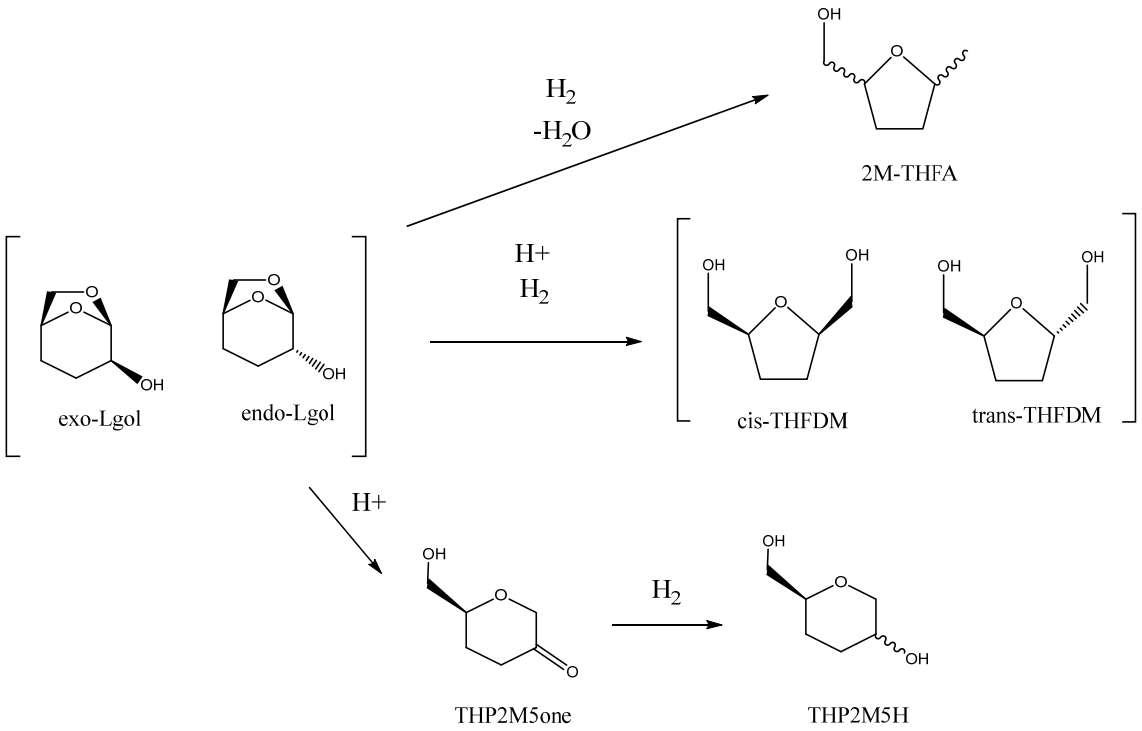

Scheme 3: Proposed reaction network for Lgol hydrogenolysis.

3.3.1. Effect of metal and acid sites

As shown in Table 2, Lgol was unreactive in the presence of a 1% Pd/Al_2O_3 catalyst at 150°C, indicating that acid sites are necessary for Lgol hydrogenolysis. Using the pure Si-Al support resulted in 32% Lgol conversion. Low selectivity (19%) was observed to THP2M5one, a product of acid-catalyzed Lgol isomerization. A physical mixture of 1% Pd/Al_2O_3 and Si-Al resulted in lower conversion (41%) and lower THFDM selectivity (29%) compared to the Pd/Si-Al catalyst (90% conversion, 58% THFDM selectivity), indicating that close proximity of metal (Pd) and acid (Si-Al) sites[26,27] is favorable for this reaction. Acid catalysts are known to carry out ring rearrangement reactions by protonating ether oxygen atoms to facilitate C-O bond cleavage.[28] Downstream hydrogenolysis products of THFDM, such as 1,2,6-hexanetriol, were not observed. The selectivities to identified products do not add to 100% when pure Si-Al support (19%) or a physical mixture of Pd/Al_2O_3 and Si-Al (48%) are used, indicating the formation of unaccounted degradation products in these cases.

Table 2. Lgol Hydrogenolysis

		Selectivity [%]				
Catalyst	**Conversion [%]**	**Cis-THFDM**	**Trans-THFDM**	**2MTHFA**	**THP2M5one**	**THP2M5H**
1% Pd/Si-Al	89.9	42.5	15.4	17.1	3.4	20.1
1% Pd/Al_2O_3	0	-	-	-	-	-
Si-Al	31.7	0	3.4*	0	18.9	0
1% Pd/Al_2O_3 + Si-Al	40.9	17.4	11.7	0	0	18.6

Conditions: 150°C, 500 psi H_2, 10 mL 60 mM Lgols in THF (exo/endo = 1.7), 100 mg cat, 3h reaction time. Si-Al calcined at 400°C prior to reaction.
**The reported selectivity towards THFDM over the Si-Al catalyst is most likely an impurity, as no metal sites are present to carry out hydrogenolysis.*

3.3.2. Selectivity versus conversion

The reaction network for Lgol hydrogenolysis was further investigated by carrying out sampling from a batch reactor over time. As calculated from Figure 3, the selectivity of Lgol conversion to THFDM was ~55% and was not a strong function of conversion. Because the selectivities to the side-products 2MTHFA and THP2M5H were also not strong functions of conversion, these products are produced in parallel with THFDM rather than in series (Scheme 3). A separate experiment with THFDM as feedstock (10 mL 60 mM THFDM feed, cis/trans = 4.8) at the same reaction conditions (150°C, 500 psi H_2, 50 mg 1% Pd/Si-Al, 3h reaction time) displayed near-zero conversion with small amounts of 2MTHFA produced (4% yield), providing further evidence that the dominant pathway for 2MTHFA formation is in parallel with THFDM rather than in series. The concentration of THP2M5one is nearly zero throughout the reaction. Based on the data in Figure 3, the initial turnover frequency (TOF) for Lgol hydrogenolysis to THFDM at these conditions was 0.84 mol THFDM per mol surface Pd per min. Catalyst recycling data suggest that this catalyst undergoes deactivation under these conditions similar to the case of LGO hydrogenation (Supplemental Information, Figure S8). The carbon balance decreased to ~85% during the reaction, indicating that minor degradation reactions are occurring at these reaction conditions.

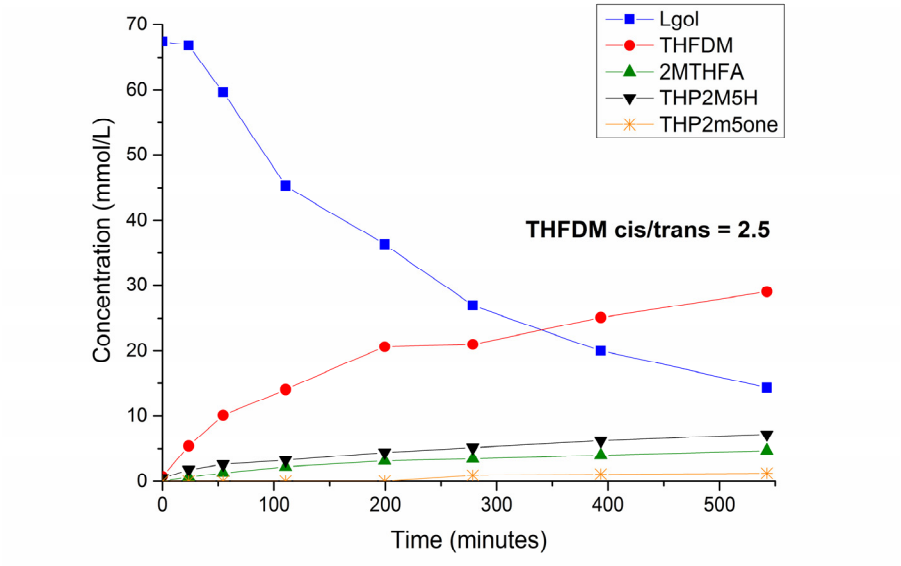

Figure 3. Hydrogenolysis of Lgol (exo/endo = 1.7) over 450 mg 1 wt% Pd/Si-Al in a batch reactor with dip-tube sampling. Conditions: 150°C, 500 psi H_2, 60 mL 60 mM Lgol in THF feed. Solid lines between points are visual aids.

3.3.3. Effect of Lgol stereochemistry

We investigated the relationship between the Lgol feedstock stereoisomer ratio and the THFDM product stereoisomer ratio. We produced a Lgol feedstock containing an exo/endo ratio of 4.7 using 0.4 wt% Pd/Al_2O_3 catalyst (Figure 2). When the Lgol hydrogenolysis reaction was carried out using this feedstock (Figure 4), the THFDM product stereoisomer ratio was nearly equal to the ratio obtained in the experiment shown in Figure 3 (cis/trans = 2.5 vs cis/trans = 2.6). This result indicates that the mechanism of Lgol hydrogenolysis to THFDM passes through an intermediate which erases the stereochemistry of the feed. Furthermore, when THFDM (cis/trans = 4.8) was fed over the Pd/Si-Al catalyst at the same reaction conditions (as discussed above), the THFDM stereoisomer ratio did not change. This result indicates that THFDM production is irreversible, and the THFDM stereoisomer ratio is governed by kinetics rather than thermodynamics.

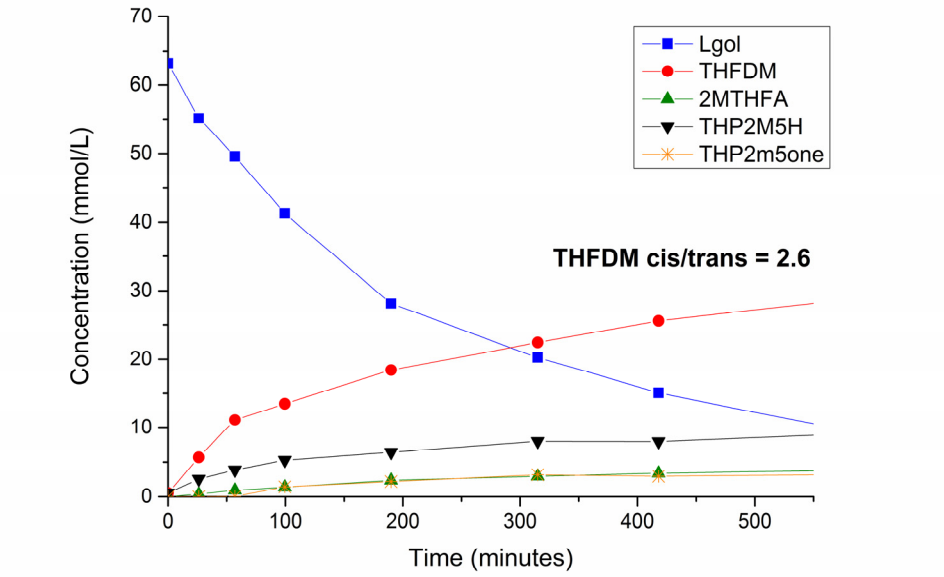

Figure 4. Hydrogenolysis of Lgol (exo/endo = 4.5) over 450 mg 1 wt% Pd/Si-Al in a batch reactor with dip-tube sampling. Conditions: 150°C, 500 psi H_2, 60 mL 60 mM Lgol in THF feed. Solid lines between points are visual aids.

3.3.4. Determining whether THP2M5one is a THFDM precursor

THP2M5one can be produced from the acid-catalyzed isomerization of Lgol in the absence of a metal catalyst, via cleavage of the C-O bond of the anhydro-bridge. Amberlyst 70, a solid acid catalyst, was used to generate a product mixture containing 30.8 mM Lgol and 21.7 mM THP2M5one (see Supplemental Information), and this mixture was fed over a Pd/Si-Al catalyst (Figure 5) to determine whether THP2M5one is an intermediate between Lgol and THFDM. An additional experiment with pure Lgol at a similar initial concentration (29.8 mM) was conducted to provide a direct comparison (Figure 6).

The THFDM concentrations over time are comparable in Figures 5 and 6. If it is assumed that Lgol is the sole precursor to THFDM, the selectivity of Lgol to THFDM is nearly identical in Figure 5 (63%) versus Figure 6 (59%). In contrast, the THP2M5H concentration is significantly higher in Figure 5 than in Figure 6. If it is assumed that the THP2M5one present in Figure 5 is just hydrogenated to THP2M5H, and additionally that the Lgol in Figure 5 is converted to THP2M5H in 35% selectivity (as in Figure 6), then the selectivity of THP2M5one conversion to THP2M5H in Figure 5 is 88%. These results indicate that THP2M5one is hydrogenated to THPM2H and is not a THFDM precursor (Scheme 3). We note that we cannot rule out the possibility of a second route from Lgol to THP2M5H which does not pass through THP2M5one. Because the 2MTHFA concentrations are comparable in Figures 5 and 6, 2MTHFA is not produced through THP2M5one or THP2M5H.

It should be noted that the product deconvolution methods are likely to be subject to greater error when the concentrations of cis-THFDM and THP2M5one are comparable (see Supplemental Information), as in Figure 5. One potential source of error is in the assumption that the GC

sensitivities of THP2M5one and Lgol are equal. Any error in the measured concentration of THP2M5one would translate to an error in the concentration of THFDM. However, small errors in the THP2M5one and THFDM concentrations would not affect the interpretation of Figure 5.

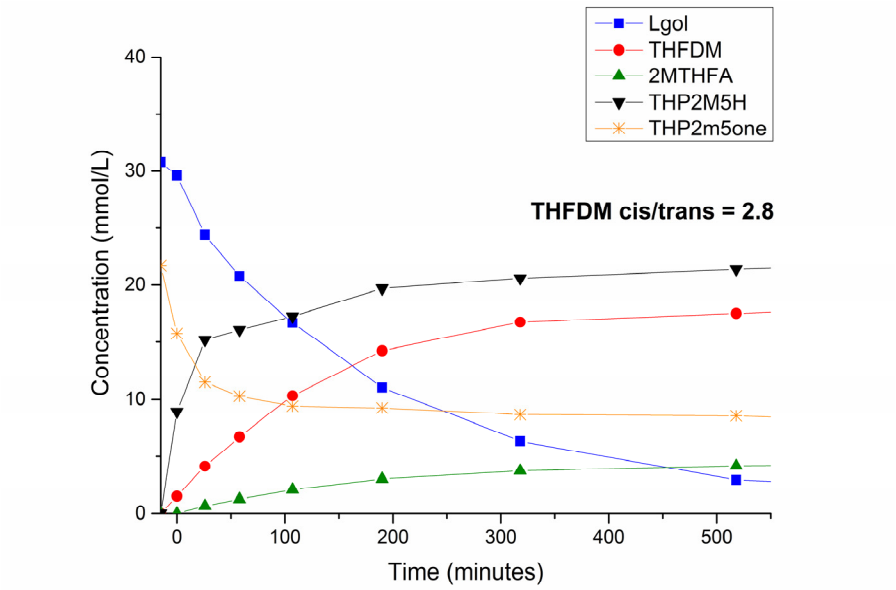

Figure 5. Hydrogenolysis of a feedstock containing THP2M5one and Lgol, over 450 mg 1 wt% Pd/Si-Al in a batch reactor with dip-tube sampling. Conditions: 150°C, 500 psi H_2, 60 mL feed containing 30.8 mM Lgol and 21.7 mM TH2m5one in THF. Time zero defined as time when the reaction temperature was reached. Solid lines between points are visual aids.

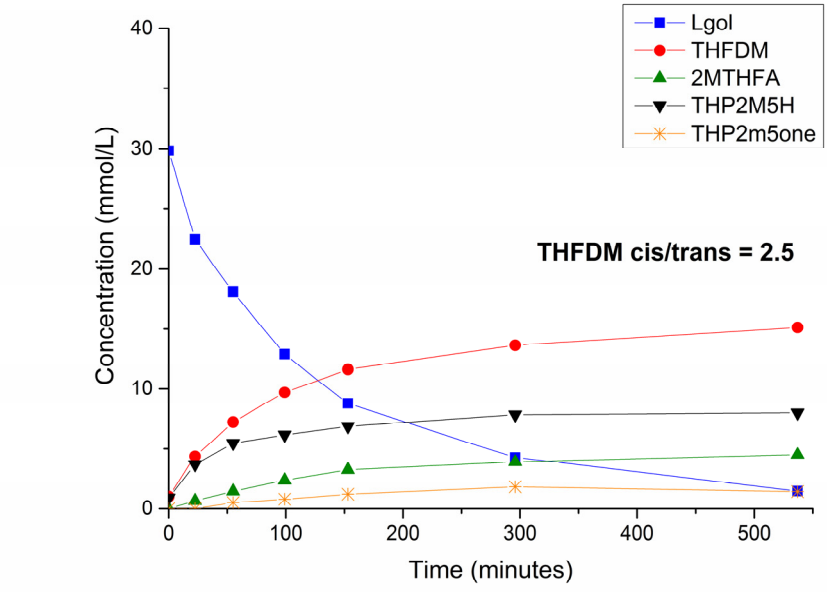

Figure 6. Hydrogenolysis of Lgol (exo/endo = 1.7) over 450 mg 1 wt% Pd/Si-Al in a batch reactor with dip-tube sampling. Conditions: 150°C, 500 psi H_2, 60 mL 30 mM Lgol in THF feed. Solid lines between points are visual aids.

3.3.5. Proposed mechanism

A mechanism for the hydrogenolysis of Lgol to THFDM that is consistent with the above findings is shown in Scheme 4. The above experiments show that Lgol hydrogenolysis does not proceed through initial isomerization of Lgol to THP2M5one, nor through the hydrogenated side-product THP2M5H. We suggest that the mechanism proceeds through initial cleavage of the anhydro-bridge of Lgol to form a surface intermediate containing a single 6-membered ring. This species could potentially be a partially hydrogenated intermediate as shown in Scheme 4.

Secondly, this species is ring-opened via protonation of the pyran ring oxygen to form an acyclic surface intermediate, similar to the hydrogenolysis of tetrahydropyran-2-methanol (THP2M) to 1,6-hexanediol.[28] The observation that the stereochemistry of the Lgol feed is erased in this reaction supports the hypothesis that the ring rearrangement occurs through an acyclic intermediate which contains only one chiral center, as opposed to a concerted ring rearrangement (we note that loss of the hydrogen atom at the C_5 position of Lgol is another way to erase the stereochemistry of the feed). Ring rearrangement occurs via nucleophilic attack of the carbocation at the C_5 position by the alcohol oxygen at the C_2 position. The stereochemistry of THFDM is determined by the spatial direction of this ring closure step. Ring closure from the less hindered direction results in the cis-THFDM configuration, consistent with the observation that a 2.5:1 ratio of cis-THFDM to trans-THFDM is observed. The observation that close proximity of metal and acid sites promotes this reaction suggests that the hydrogen atom addition and ring rearrangement steps may need to occur in concert in order to carry out this reaction effectively.

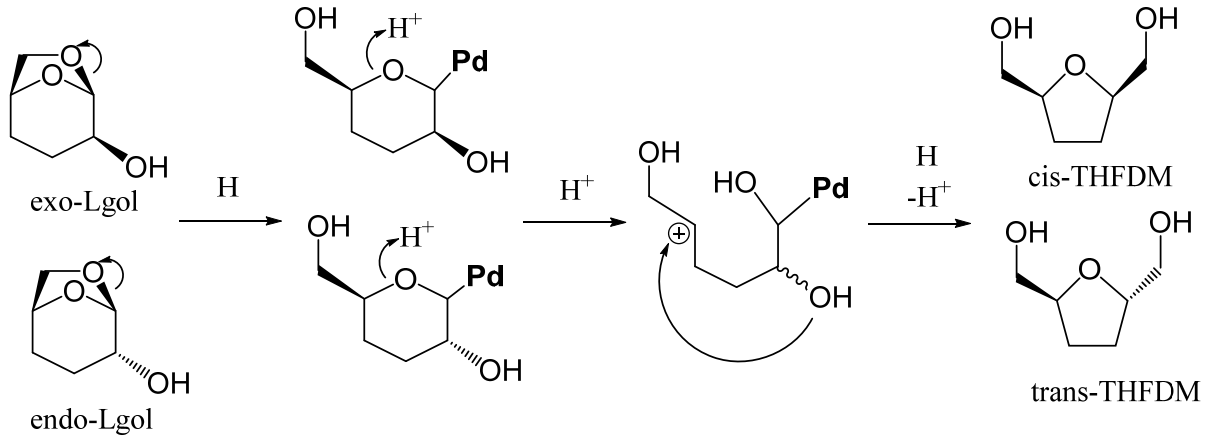

Scheme 4: Proposed mechanism for Lgol hydrogenolysis to THFDM

4. Conclusions

We have shown that LGO can be selectively hydrogenated to Cyrene at low temperature (40°C), and further hydrogenated to two stereoisomers of Lgol at higher temperatures (100°C). An excess of the exo-Lgol isomer is favored over supported Pd catalysts across multiple particle sizes and temperatures, and the stereoisomer ratio is kinetically controlled. Lgol can be further upgraded to THFDM at 150°C in 58% selectivity over a bifunctional Pd/Si-Al catalyst, with an overall selectivity of 78% to 1,6-hexanediol precursors. An excess of cis-THFDM to trans-THFDM was produced over Pd/Si-Al, independent of the stereoisomer ratio of the Lgol feedstock, suggesting that the initial stereochemistry at the alcohol position of Lgol is erased during the reaction.

Although THP2M5one can be produced from the acid-catalyzed isomerization of Lgol, THP2M5one is hydrogenated to THP2M5H, and neither of these species are THFDM precursors. Our results demonstrate that LGO has the potential to become a platform molecule used for the production of high-value oxygenated chemicals, such as Cyrene, Lgol, or THFDM, from lignocellulosic biomass.

5. Acknowledgements

This material is based upon work supported by the Department of Energy, Office of Energy Efficiency and Renewable Energy (EERE), under Award Number DE-EE0006878. S.H.K. acknowledges that this material is based upon work supported by the National Science Foundation under Grant No. DGE-1256259. We thank the UW-Madison Department of Chemistry for use of Bruker Avance 500 MHz NMR Spectrometer. A generous gift from Paul J. Bender enabled this spectrometer to be purchased [2012].

6. References

1. G. W. Huber, S. Iborra and A. Corma, *Chemical Reviews*, 2006, **106**, 4044-4098.
2. J. N. Chheda, G. W. Huber and J. A. Dumesic, *Angewandte Chemie International Edition*, 2007, **46**, 7164-7183.
3. F. Cao, T. J. Schwartz, D. J. McClelland, S. H. Krishna, J. A. Dumesic and G. W. Huber, *Energy & Environmental Science*, 2015, **8**, 1808-1815.
4. H. Kawamoto, S. Saito, W. Hatanaka and S. Saka, *Journal of Wood Science*, 2007, **53**, 127-133.
5. F. Shafizadeh, R. H. Furneaux and T. T. Stevenson, *Carbohydrate Research*, 1979, **71**, 169-191.
6. J. Sherwood, M. De bruyn, A. Constantinou, L. Moity, C. R. McElroy, T. J. Farmer, T. Duncan, W. Raverty, A. J. Hunt and J. H. Clark, *Chemical Communications*, 2014, **50**, 9650-9652.
7. M. De bruyn, J. Fan, V. L. Budarin, D. J. Macquarrie, L. D. Gomez, R. Simister, T. J. Farmer, W. D. Raverty, S. J. McQueen-Mason and J. H. Clark, *Energy & Environmental Science*, 2016, **9**, 2571-2574.
8. J. Zhang, G. White, M. Ryan, A. J. Hunt and M. J. Katz, *ACS Sustainable Chemistry & Engineering*, 2016.
9. *USA Pat.,* US 8865,940 B2, 2014.
10. T. Buntara, I. Melián-Cabrera, Q. Tan, J. L. G. Fierro, M. Neurock, J. G. de Vries and H. J. Heeres, *Catalysis Today*, 2013, **210**, 106-116.
11. T. Buntara, S. Noel, P. H. Phua, I. Melián-Cabrera, J. G. de Vries and H. J. Heeres, *Topics in Catalysis*, 2012, **55**, 612-619.
12. T. Buntara, S. Noel, P. H. Phua, I. Melián-Cabrera, J. G. de Vries and H. J. Heeres, *Angewandte Chemie International Edition*, 2011, **50**, 7083-7087.
13. M. R. Nolan, G. Sun and B. H. Shanks, *Catalysis Science & Technology*, 2014, **4**, 2260-2266.
14. M. M. Zanardi and A. G. Suárez, *Tetrahedron Letters*, 2009, **50**, 999-1002.
15. C. Moreau, M. N. Belgacem and A. Gandini, *Topics in Catalysis*, 2004, **27**, 11-30.
16. 1,6-Hexanediol Market by Application (Polyurethanes, Coatings, Acrylates, Adhesives, Unsaturated Polyester Resins, Plasticizers, and Others) and By Geography (NA, Europe,

Asia-Pacific, & ROW) - Trends and Forecasts to 2019, http://www.researchandmarkets.com/research/zs4gnb/16hexanediol, (accessed January 22, 2016).
17. S. Van de Vyver and Y. Roman-Leshkov, *Catalysis Science & Technology*, 2013, **3**, 1465-1479.
18. P. Werle, M. Morawietz, S. Lundmark, K. Sörensen, E. Karvinen and J. Lehtonen, in *Ullmann's Encyclopedia of Industrial Chemistry*, Wiley-VCH Verlag GmbH & Co. KGaA, 2000.
19. B. Xiao, M. Zheng, X. Li, J. Pang, R. Sun, H. Wang, X. Pang, A. Wang, X. Wang and T. Zhang, *Green Chemistry*, 2016, **18**, 2175-2184.
20. J. Tuteja, H. Choudhary, S. Nishimura and K. Ebitani, *ChemSusChem*, 2014, **7**, 96-100.
21. R. Alamillo, M. Tucker, M. Chia, Y. Pagan-Torres and J. Dumesic, *Green Chemistry*, 2012, **14**, 1413-1419.
22. E. Ronzón and G. Del Angel, *Journal of Molecular Catalysis A: Chemical*, 1999, **148**, 105-115.
23. P. Mäki-Arvela, J. Hájek, T. Salmi and D. Y. Murzin, *Applied Catalysis A: General*, 2005, **292**, 1-49.
24. R. L. Augustine, *Catalysis Today*, 1997, **37**, 419-440.
25. X. Hu, R. J. M. Westerhof, L. Wu, D. Dong and C.-Z. Li, *Green Chemistry*, 2015, **17**, 219-224.
26. F. Leydier, C. Chizallet, A. Chaumonnot, M. Digne, E. Soyer, A.-A. Quoineaud, D. Costa and P. Raybaud, *Journal of Catalysis*, 2011, **284**, 215-229.
27. E. J. M. Hensen, D. G. Poduval, P. C. M. M. Magusin, A. E. Coumans and J. A. R. v. Veen, *Journal of Catalysis*, 2010, **269**, 201-218.
28. M. Chia, Y. J. Pagán-Torres, D. Hibbitts, Q. Tan, H. N. Pham, A. K. Datye, M. Neurock, R. J. Davis and J. A. Dumesic, *Journal of the American Chemical Society*, 2011, **133**, 12675-12689.
29. M. J. Frisch, G. W. Trucks, H. B. Schlegel, G. E. Scuseria, M. A. Robb, J. R. Cheeseman, G. Scalmani, V. Barone, B. Mennucci, G. A. Petersson, H. Nakatsuji, M. Caricato, X. Li, H. P. Hratchian, A. F. Izmaylov, J. Bloino, G. Zheng, J. L. Sonnenberg, M. Hada, M. Ehara, K. Toyota, R. Fukuda, J. Hasegawa, M. Ishida, T. Nakajima, Y. Honda, O. Kitao, H. Nakai, T. Vreven, J. A. Montgomery Jr., J. E. Peralta, F. Ogliaro, M. J. Bearpark, J. Heyd, E. N. Brothers, K. N. Kudin, V. N. Staroverov, R. Kobayashi, J. Normand, K. Raghavachari, A. P. Rendell, J. C. Burant, S. S. Iyengar, J. Tomasi, M. Cossi, N. Rega, N. J. Millam, M. Klene, J. E. Knox, J. B. Cross, V. Bakken, C. Adamo, J. Jaramillo, R. Gomperts, R. E. Stratmann, O. Yazyev, A. J. Austin, R. Cammi, C. Pomelli, J. W. Ochterski, R. L. Martin, K. Morokuma, V. G. Zakrzewski, G. A. Voth, P. Salvador, J. J. Dannenberg, S. Dapprich, A. D. Daniels, Ö. Farkas, J. B. Foresman, J. V. Ortiz, J. Cioslowski and D. J. Fox, *Gaussian 09, Revision C.01,* Gaussian, Inc.: Wallingford, CT, 2009.
30. NIST Chemistry WebBook, http://webbook.nist.gov/, (accessed 10/1/16, 2016).
31. D. W. Rogers, Y. Zhao, M. Traetteberg, M. Hulce and J. Liebman, *The Journal of Chemical Thermodynamics*, 1998, **30**, 1393-1400.
32. M. S. Miftakhov, I. N. Gaisina, F. A. Valeev and O. V. Shitikova, *Russian Chemical Bulletin*, 1995, **44**, 2350-2352.

33. T. J. Connolly, J. L. Considine, Z. Ding, B. Forsatz, M. N. Jennings, M. F. MacEwan, K. M. McCoy, D. W. Place, A. Sharma and K. Sutherland, *Organic Process Research & Development*, 2010, **14**, 459-465.
34. A. Tagirov, I. Biktagirov, Y. Galimova, L. Faizullina, S. Salikhov and F. Valeev, *Russian Journal of Organic Chemistry*, 2015, **51**, 569-575.